chemistry

MDPI

Article

Durable Polymer Coatings: A Comparative Study of PDMS-Based Nanocomposites as Protective Coatings for Stone Materials

Maduka L. Weththimuni [1,*], Marwa Ben Chobba [2], Donatella Sacchi [1], Mouna Messaoud [2] and Maurizio Licchelli [1]

[1] Department of Chemistry, University of Pavia, Via Taramelli 12, 27100 Pavia, Italy; donatella.sacchi@unipv.it (D.S.); maurizio.licchelli@unipv.it (M.L.)
[2] Laboratory of Advanced Materials, National School of Engineering, University of Sfax, P.O. Box 1173, Sfax 3038, Tunisia; marwa.benchobba@enis.tn (M.B.C.); mouna.messaoud@enis.tn (M.M.)
* Correspondence: madukalankani.weththimuni@unipv.it

Abstract: Nowadays, durable protective coatings receive more attention in the field of conservation for several reasons (they are cost effective, time consuming, more resistance, etc.). Hence, this study was focused on producing a multi-functional, durable coating to protect different stone materials, especially, Lecce stone, bricks, and marble. For this purpose, ZrO_2-doped-ZnO-PDMS nanocomposites (PDMS, polydimethylsiloxane used as the binder) were synthesized by in situ reaction (doped nanoparticles were inserted into the polymer matrix during the synthesis of PDMS) and the performances of resulting coatings were examined by handling different experimental analyses. In particular, the study aimed to evaluate the durability properties of the coating along with the self-cleaning effect. As a result, the durability of the nanocomposite coating with respect to the well-known PDMS coating was assessed after exposure to two different ageing cycles: solar ageing (300 W, 1000 h) and humid chamber ageing (RH > 80%, T = 22 ± 3 °C, desiccator, 2 years). All the results were in good agreement with each other providing that newly prepared nanocomposite coating can be used as a durable protective coating for different stone materials.

Keywords: durability; nanocomposite coating; ZrO_2-doped-ZnO-PDMS; ageing cycles; self-cleaning effect

Citation: Weththimuni, M.L.; Chobba, M.B.; Sacchi, D.; Messaoud, M.; Licchelli, M. Durable Polymer Coatings: A Comparative Study of PDMS-Based Nanocomposites as Protective Coatings for Stone Materials. *Chemistry* **2022**, *4*, 60–76. https://doi.org/10.3390/chemistry4010006

Academic Editor: M. Alejandro Presa Soto

Received: 27 December 2021
Accepted: 27 January 2022
Published: 29 January 2022

1. Introduction

The preservation of artifacts is an important and essential endeavor due to the deterioration phenomena, which is happening for several reasons (physical, chemical, and biological agents). The direct exposure of any type of stone materials, particularly the most porous ones, may cause physicochemical changes of the substrate, resulting in aesthetic deformation and disfiguration of superficial decoration (e.g., the formation of black crusts) and bio–geophysical and bio–geochemical damage [1–3]. Taking into consideration all the deterioration factors, scientists have focused their research on finding new materials and new methodologies to overcome these problems.

In recent years, the application of nanotechnology to the field of Cultural Heritage has made a great contribution to colloid and interface science, to material science, and to conservation science [1,4]. In particular, many new materials based on the proper handling of nano-sized components have been developed, which display better performance (e.g., higher reactivity, higher durability, and easy application) than other corresponding traditional materials.

In the field of cultural heritage conservation, many protective and consolidation products have been developed using nanomaterials [5–12]. Moreover, conservation experts show great interest in producing new products, which are able to achieve higher surface

protection, consolidation, and self-cleaning efficiencies [13–16]. For instance, C. Kapridaki et al. have synthesized a photo-active, transparent and hydrophobic SiO_2-crystalline TiO_2 nanocomposites coating for marble [15]; the same group has reported a TEOS-nano-calcium oxalate consolidant and TEOS-PDMS-TiO_2 hydrophobic/photoactive, hybrid nanomaterials for different stone types [17]; M. F. La Russa et al. have analyzed the hydrophobic and the self-cleaning efficacy of nano-TiO_2 coatings with different binder materials for cultural heritage protection [18]; V. Crupi et al. have discussed the optimal amounts of TiO_2 NPs contained in the nanocomposite coating of TiO_2–SiO_2–PDMS as a self-cleaning coating for stone material [16]; M. Luna et al. have examined the self-cleaning effect of low content of Au NPs inside TiO_2-SiO_2 coatings for building materials [19]; S. Banerjee et al. have reported the applications of TiO_2 as a self-cleaning coating [20]; M. Ben Chobba et al. have recently discussed the self-cleaning and antibacterial effect of Ag-TiO_2/PDMS nanocomposite protective coatings for Lecce stone [13]. As can be seen in the literature, most authors have used TiO_2 NPs, which have been properly modified, for instance by doping them with another nano-sized materials, in order to improve the well-known photocatalytic properties displayed by Titania NPs and the resulting self-cleaning effect.

After considering all these studies reported in the literature, we have investigated the photocatalytic effectiveness of semi-conductive materials other than TiO_2, for instance zinc oxide. ZnO has been studied for many applications, especially in optics and electronics areas due to its excellent properties, such as being a UV absorber, low cost, non-toxic, inert color, easy application, and environmental friendliness. Moreover, nano-sized ZnO also in combination with different binders has been proposed in some conservation treatments for cultural heritage [21–25]. In this research study, we considered how to improve the photocatalytic activity of ZnO NPs by using an inorganic dopant. As reported in the literature, the process of doping can alter the surface reactivity, functionality and charge of the NPs, with possible improvement of their properties such as durability, stability, and dispersive ability of core material [26,27]. As a dopant, we choose Zirconium dioxide (ZrO_2), which is a P-type semiconductor, with a wide band gap, and is used in many fields due to its excellent properties including good natural color, high strength, high toughness, high chemical stability, and chemical and microbial resistance [27,28].

Great interest has been (and is currently) devoted by the conservation scientists towards multi-functional and durable coatings based on nanomaterials with potential application in the protection of artifacts from several decaying factors, owing to some promising features such as high resistance to decay, long term durability, harmlessness, and cost effectiveness [14,18]. Concerning multi-functional coatings with specific application in the protection of stone substrates, they also exhibit additional important features, such as homogeneous distribution on the stone matrix, appropriate thickness, good water repellent behavior, acceptable level of permeability to vapor, good hardness, self-cleaning properties, and long-term durability. Therefore, we focused our interest on the preparation of a multi-functional coating using ZnO NPs properly doped with ZrO_2 NPs. Polydimethylsiloxane (PDMS) was selected as a polymeric binder as it has been widely used in the protection of stone substrate as well as to prepare other multi-functional coatings containing inorganic NPs [13–17]. A preliminary study about the performance of this nanocomposite coating has been already reported [27]. In the present work investigation has been mainly focused on durability that represents a key property when considering protecting coatings for stone substrates.

For this purpose, the nanocomposite coating (ZrO_2-ZnO-PDMS) was examined when applied on three different stone types, i.e., Lecce stone (LS), brick (B) and Carrara marble (M). The selected stones have totally different chemical compositions and their open porosities are also very different to each other. Therefore, the performances of this newly prepared nanocomposite coating were investigated on totally different stones, taking into account that protective features are highly affected by substrate structure. The stone specimens treated with just the polymer (PDMS) were used as the reference for each and every analyses.

The effects induced by nanocomposite application on the stone surface have been preliminary assessed (contact angles and chromatic variation measurements, capillary absorption and water vapor permeability determinations) in our previous paper [27]. The nanocomposite coating was further analyzed by different techniques in order to better understand its properties. In particular: chemical structure and PDMS–NPs interactions were examined by the FTIR (ATR mode) technique; morphological and microstructural features were analyzed by an optical microscope (UV light) and scanning electron microscopy (SEM, backscattered electron) and energy-dispersive X-ray spectra (EDS); the surface hardness due to the coatings was measured using the international standard test, and photodegradation efficiency (self-cleaning ability) was examined by handling methylene blue (MB) dye degradation test under UV light irradiation. Moreover, the durability analysis was conducted by artificially ageing the stone specimens using two different methods: solar light irradiation (300 W, 1000 h), and humid chamber ageing in the laboratory (RH > 80%, T = 22 ± 3 °C, desiccator, 2 years). At the end of both ageing cycles, all the changes of treated stone specimens due to ageing were thoroughly investigated by measuring the chromatic variations, contact angle, surface hardness, and self-cleaning efficiency.

2. Materials and Methods

2.1. Materials

Ethanol (absolute, 99.8% EtOH), sodium hydroxide (NaOH), zinc acetate dihydrate ($ZnC_4H_6O_4{\cdot}2H_2O$), 2-propanol, zirconium oxychloride octahydrate, tert-Butyl alcohol (TBA, $C_4H_{10}O$, 99.7%), hexamethyldisiloxane, orthophosphoric acid, and octamethylcyclotetrasiloxane (D_4, utilized as PDMS precursor) were purchased from Sigma-Aldrich (St. Louis, MO, USA). Cesium hydroxide ($CsOH{\cdot}H_2O$) was purchased from Alfa Aesar (Haverhill, MA, USA). All the chemicals were of analytical grade and used without further purification. Water was purified using a Millipore Organex system: R ≥ 18 M cm (Burlington, MA, USA). Lecce stone specimens were provided by Tarantino and Lotriglia (Nardò, Lecce, Italy), while specimens of brick and Carrara marble were provided by Favret Mosaici S.a.s. (Pietrasanta, Lucca, Italy).

2.2. Synthesis of Nanoparticles

ZrO_2-ZnO core–shell NPs (molar ratio about 0.01:1 ZrO_2/ZnO) were synthesized by the sol–gel method reported in the literature [26,28,29]. First of all, ZnO NPs were synthesized using NaOH and zinc acetate dehydrate as follows [23]. NaOH dissolved in EtOH (50 mL, 0.3 M) was added dropwise into a round bottom flask containing a solution of $Zn(CH3COO)_2$ in EtOH (50 mL, 0.2 M) with continuous magnetic stirring. The resulting mixture was heated, and a white precipitate formed when the temperature reached 78.4 °C. After that, the solid product was washed several times with water and then with absolute EtOH. Finally, the product obtained was dried in an oven at 150 °C for several hours in order to obtain ZnO nanopowder. After that, 0.5 g of ZnO NPs were dispersed in 20 mL EtOH and poured into a three-neck round bottom flask. From one neck of the flask, an aqueous solution of $ZrOCl_2{\cdot}8H_2O$ (50 mL, 0.1 M) was added dropwise, while the other neck was used to introduce dropwise a NaOH aqueous solution (15 mL, 1 M), and the reaction mixture was continuously stirred by magnetic stirring. The temperature of the resulting mixture was set at 80 °C and, after obtaining a white precipitate, it was centrifuged and washed with deionized water and EtOH and then dried in an oven at 150 °C for several hours [23,28].

The ZrO_2-ZnO-PDMS nanocomposite (NPs: PDMS ratio 0.5% (*w*/*w*)) was prepared by the in situ reaction. For this purpose, doped NPs (0.125 g) were introduced to the reaction mixture containing octamethylcyclotetrasiloxane (D_4, 25 g) with tert-Butyl alcohol 20 mL and CsOH (0.15 g), used as a catalyst for the ring opening polymerization of D_4. After ultrasonication (20 min), the reaction was carried out at 120 ± 3 °C under vigorous stirring for 2.5 h in an oil bath, and then hexamethyldisiloxane (0.03 g) was added and the reaction was continued at the same temperature another 2.5 h, as recommended in the

literature [26]. Then, it was cooled to room temperature and the unreacted D_4 was removed by distillation after degassing. Orthophosphoric acid was slowly added to the reaction container under continuous stirring to neutralize any unreacted CsOH. Afterwards, the solution was allowed to stand for one day, and then the product was subsequently filtrated for removing the solvents. Plain PDMS was prepared with the same reaction (without NPs).

2.3. Preparation of Stone Samples and Their Coating Applications

All the stone specimens were cleaned before the treatments following the standard method (UNI 10,921 Protocol) [30]. Lecce stone (LS), brick (B), and marble (M) specimens (squared 5 × 5 × 1 and 5 × 5 × 2 cm) were smoothed by abrasive, carbide paper (No: 180 mesh), washed with deionized water, dried in an oven at 60 °C and stored in a desiccator until they reach room temperature, then their dry weight was measured until it was constant [6,8,31].

After cleaning all the stone specimens, they are ready for coating applications. Hence, all considered samples were treated with ZrO_2-ZnO-PDMS nanocomposite (named as Zr-Zn-P) as well as with plain PDMS (named as P, as the reference) by the brushing method (applied amount, 1.0 ± 0.02 g for each specimen). Specimens treated with the nanocomposite were named Zn-Zr-P_LS, Zn-Zr-P_B, and Zn-Zr-P_M, while reference specimens were labeled P_LS, P_B, and P_M.

2.4. Experimental Techniques and Methods

All the treated stone specimens were analyzed by using different techniques as follows. Chromatic variations were measured by a Konica Minolta CM-2600D spectrophotometer (Konica Minolta, Inc., Tokyo, Japan), determining the L^*, a^*, and b^* coordinates of the CIELAB space, and the global chromatic variations, expressed as ΔE^* according to the UNI EN 15886 protocol [32]. In order to calculate the average value, five measurements on each specimen were performed and these were conducted on three specimens of each kind of treatment in every stone type, so all the given results are average values from 15 different measurements.

The hydrophobic property of the new coating with respect to the polymer coating was examined by static contact angle measurements. It was measured by a Lorentzen and Wettre instrument (Zurich, Switzerland) according to the UNI EN 15802 Protocol [33]. The average values were taken from 15 measurements of each coating.

The water suction through capillarity was performed to examine the water absorption capacity of coatings through the stone substrates. The amount of absorbed water as a function of time was set on the 5 × 5 × 2 cm of each and every stone specimen (three specimens of each kind of treatment of each stone type were used to obtain the average value) according to the UNI EN 15801 Protocol [34]. Furthermore, the Qf reflects the amount of water absorbed after 96 h (at the end of the experiment).

The water vapor transmissions of the treated and untreated stone material were evaluated at 20 °C by performing a permeability test on the 5 × 5 × 1 cm each stone specimen according to the UNI EN 15803:2010 protocol [35]. The average values were obtained from three different samples of each kind of stone as explained in the other experimental analyses.

Infrared spectra were collected by a PerkinElmer Spectrum 100 Fourier transform infrared (FT-IR) spectrometer in the attenuated total reflectance (ATR) mode (PerkinElmer, Waltham, MA, USA).

Optical microscopy observations of the treated specimens were conducted using a light polarized microscope Olympus BX51TF, equipped with the Olympus U-RFL-T (UV light) (Olympus Corporation, Tokyo, Japan).

Scanning electron microscopy (SEM) images (backscattered electron) and energy-dispersive X-ray spectra (EDS) were collected by using a Tescan FE-SEM, MIRA XMU series (TESCAN, Brno, Czech Republic), equipped with a Schottky field emission source, and with a Bruker Quantax 200 energy-dispersive X-ray spectrometer (Bruker, Billerica,

MA, USA), operating in both low and high vacuum, and located at the Arvedi Laboratory, CISRiC, University of Pavia, Pavia, Italy.

The pencil hardness test was performed on all the treated stone specimens, according to the ISO15184:1998 standard (here, the scale ranging between "9B (softer)–9H (harder)" and the intermediate is "F" [36]. The obtained results are an average of three different measurements.

The self-cleaning efficiency of the newly synthesized coating with respect to the polymer coating (PDMS) was evaluated by a handling photodegradation test under UV irradiation. For this purpose, the MULTIRAYS photochemical reactor (HepatoChem Inc, Beverly, MA, USA), composed of UV chamber equipped with 8 UV lamps (the mercury medium pressure UV lamps with peak emission in the UV-A range at 357 nm and 420 nm) was used and the power of each lamp was 15 W with a total power of 120 W. Moreover, the reactor was equipped with a rotating disc in order to ensure a homogenized light irradiation on all stained samples. The discoloration of methylene blue dye (MB, 0.1% (*w*/*w*) in ethanol solution), applied on the surface of each treated stone specimen and their untreated counterparts, was controlled by measuring chromatic variations before and after application of MB dye, after 48 and 96 h of UV exposure. The photocatalytic discoloration MB stains (D^*) over time were assessed by measuring the chromatic coordinate b^*, which is sensitive to the blue color of MB dye. D^* is defined as follows (Equation (1)) [37].

$$D^* = \frac{b^*(t) - b^*(MB)}{b^*(MB) - b^*(0)} \times 100 \quad (1)$$

where $b^*(0)$ is the value of chromatic coordinate b^* before staining, while $b^*(MB)$, and $b^*(t)$ are the mean values after the application of methylene blue over the surfaces and after t hours of UV-A light exposure, respectively.

Moreover, the photocatalytic activity of the treated stones can be evaluated using another method, in which the rates of overall chromatic variation were used to examine the discoloration effect. In particular, the ratios $\Delta E^*/\Delta E^*_0$ at different irradiation time intervals were calculated, where ΔE^*_0 expresses the total color difference between treated MB stained and treated unstained surface at a time equal to zero minutes. ΔE^* corresponds to the same measurements recorded at each irradiation time and all the calculations were conducted using the following Equations (2) and (3) [15].

$$\Delta E^*(t) = \sqrt{(L^*(t) - L^*(0))^2 + (a^*(t) - a^*(0))^2 + (b^*(t) - b^*(0))^2} \quad (2)$$

$$\Delta E^*(0h) = \sqrt{(L^*(MB) - L^*(0))^2 + (a^*(MB) - a^*(0))^2 + (b^*(MB) - b^*(0))^2} \quad (3)$$

L^*, a^*, $b^*(MB)$ and L^*, a^*, $b^*(t)$: the mean values after the application of methylene blue over surfaces and after t hours of UV-A light exposure, respectively.
$L^*(0)$, $a^*(0)$ and $b^*(0)$: the chromatic coordinates of treated stones before staining with an MB dye (the difference in between treated and untreated stone specimens).

The ageing tests were performed using two different methods: (1) nanocomposite coating and PDMS coating underwent artificial solar ageing by means of a 300 W OSRAM Ultravitalux light with an UV-A component (315–400 nm, 13.6 W) and UV-B component (280–315 nm, 3.0 W), the irradiation period lasted up to 1000 h; (2) treated stone specimens were kept in the laboratory under humid environment (RH > 80%, T = 22 ± 3 °C in a desiccator) for two years (from 2019 to 2021) [13,14].

After ageing cycles, all the stone samples aged by the two methods were stained by the MB dye in order to examine the photo-degradation efficiency of two different coatings. It is important to highlight this experiment, because the photodegradation effect was assessed after strong ageing cycles, aiming to point out the long-term efficiency. The discoloration effect was assessed by measuring the chromatic variations of MB dye under UV light irradiation as explained above.

3. Results and Discussion

3.1. Characterization of Materials

As previously reported [27], the doped NPs (ZnO-ZrO_2) have a size ranging between 15 and 30 nm and they are spherical in shape.

PDMS was synthesized by the well-known ring-opening polymerization procedure [38] using octamethylcyclotetrasiloxane (D4) as the cyclic monomer, and hexamethyldisiloxane as the chain terminator, in the presence of CsOH as the base catalyst. In order to prepare PDMS nanocomposites, anionic polymerization was carried out according to the same synthetic pathway (by using the same reagents and experimental conditions), but in the presence of doped NPs (0.5% w/w). As a result, ZnO-ZrO_2 NPs were well dispersed in the final polymer matrix. Additionally, a direct NPs involvement in the reaction could be hypothesized, as OH groups on the particles surface could take part in the siloxane condensation process. As a consequence, NPs might produce covalently bonded to the PDMS polymer chains, also inducing a cross-linking process.

FTIR analysis was conducted in order to understand the chemical structure of the newly synthesized nanocomposite coating (Zn-Zr-P). Figure 1 shows the differences in PDMS (P) chemical structure after in situ reaction with doped NPs. In the spectrum of the polymer, it is possible to note that the presence of the broadband located in the spectral region 3000–3700 cm^{-1} corresponds to the –OH stretching from the absorbed water and ethanol [39,40], while in the other spectrum, it is clear that the disappearance of the –OH band around 3500 cm^{-1} may be due to leaving of –OH groups and linking of the NPs with –Si groups. In addition, the C–H absorptions at 2931 and 2892 cm^{-1} can be seen in both spectrums due to the presence of $–CH_3$ groups [15,17,40]. Moreover, the changes of the $–Si–CH_3$ band at around 1260–1259 and 789–796 cm^{-1} and the disappearance of the Si–OH absorption peak at 895 cm^{-1} which also provide a good confirmation of the cross-linking behavior (creates covalent bonding) in between NPs and the –Si groups [40,41]. It is worth noting that the most important band of the Si–O–Si stretching band (1020–1074 cm^{-1}) changed due to the reaction [40], and the new shoulder peak appeared between 876 and 895 cm^{-1}, which may be due to the formation of Si–O–Zn bonds (see Figure 1 enlarged spectrum) [42,43]. All these behaviors indicate that PDMS correctly linked with the doped NPs in the in situ reaction as expected and it is very important to produce good nanocomposite coating properties, because, if there is a chemical bond in between NPs and the polymer materials, they can produce a more durable coating than just coating with NPs as additives.

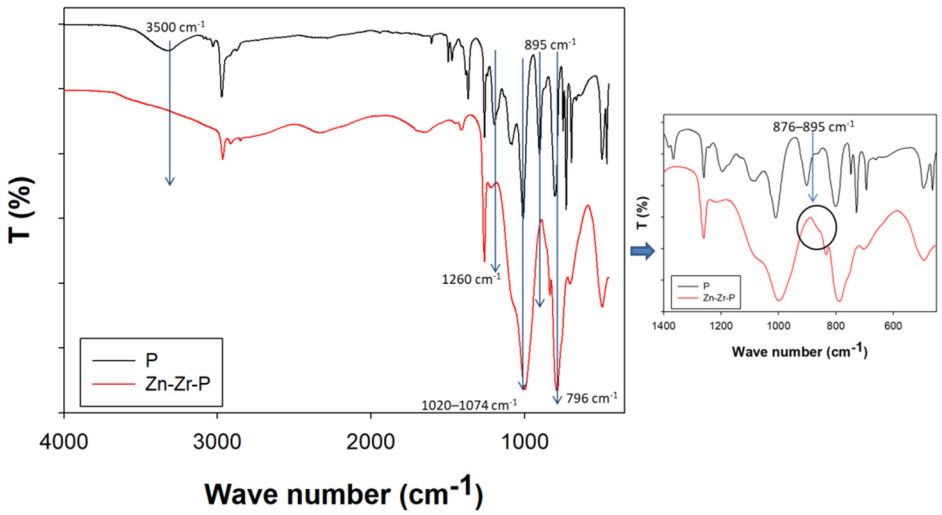

Figure 1. FTIR (ATR mode) of the synthesized nanocomposite coating compared with the PDMS coating and its enlarged spectrum of wave number between 450 cm^{-1} and 1400 cm^{-1}.

3.2. Characterization of Treated Stone Specimens

The absorbed amount of products was measured after 21 days of the treatments (Table S1 in the supplementary materials), and the highest absorption rate was observed for Lecce stone, while marble samples showed the lowest absorption. This result is in agreement with the porosity of the examined stones, which decreases in the following order: LS > B > M (LS > 30%, B~24%, and M~0.5%) [44–47]. The two applied products (P and Zn-Zr-P) were absorbed similarly by each stone substrate (regardless of the presence of NPs). As previously reported [27], both treatments (coatings of P and Zn-Zr-P) did not significantly alter the original color of any stone type, as indicated by the overall chromatic variations ($\Delta E^* < 5$, i.e., corresponding to changes that cannot be seen by the naked eye) [48]. On the other hand, we have already reported that the treated stones exhibited water repellent behavior and vapor permeability was preserved at acceptable levels compared to their counterpart untreated stones [27]. However, each stone type showed its own behavior towards water and water vapor, due to their different porosity properties. For example, Lecce stone treated by nanocomposite coating absorbed the highest amount of water by the capillary method at the end of the experiment (Qf = 434.18 ± 6.68 mg cm^{-2}), compared to brick (Qf = 263.19 ± 13.49 mg cm^{-2}) and marble (Qf ~ 10.73 ± 2.34 mg cm^{-2}) [40]. The same trend can be observed by the PDMS-treated stones (Qf_{LS} = 479.04 ± 8.16 mg cm^{-2}, Qf_B = 346.66 ± 10.49 mg cm^{-2}, and Qf_M = 15.34 ± 1.60 mg cm^{-2}). The water vapor permeability of treated stones shows the same trend, confirming that "hydric" properties highly depend on their chemical composition and porosity. Moreover, they indicated that Zn-Zr-P coating induces a small but detectable reduction in permeability (values for Zn-Zr-P: LS = 174 ± 4 g cm^{-2} 24 h, B = 95 ± 5 g cm^{-2} 24 h, and M = 15 ± 2 g cm^{-2} 24 h; for P: LS = 185 ± 6, g cm^{-2} 24 h, B = 107 ± 4 g cm^{-2} 24 h, and M = 17 ± 1 g cm^{-2} 24 h).

Contact angle measurements also indicated that all the stone surfaces show hydrophobic behavior ($\alpha > 90°$) after both treatments (P and Zn-Zr-P) [27]. Nevertheless, it is worth highlighting that the surfaces of nanocomposite-coated stones are more hydro-repellant than those coated with plain PDMS stones. In particular, the value of the contact angle increases by 20° (from PDMS to nanocomposite) in the case of LS, while it increases by more than 10° for B and M. It may be due to the homogeneous distribution of NPs in the polymer matrix and due to the possible cross-linking of the PDMS polymer induced by the presence of NPs, which results in an improved resistance to water penetration. Moreover, the results obtained from the capillary absorption test also confirmed this behavior.

Morphological and micro-structural differences due to the treatments were analyzed by optical microscopy observations and SEM-EDS experiments. As can be seen in Figure 2, some differences between the two different coatings can be pointed out by UV light. In the case of nanocomposite coating, nanoparticles well dispersed in the polymer can be clearly seen over the stone surface, especially on bricks and marble (Figure 2e,f, respectively).

The investigation of samples by SEM confirmed the homogeneous distribution of both coatings on the stone surface (Figures 3 and 4) as well as the morphological differences of the two polymeric materials applied on the stone surface. In particular, the nano-sized inorganic particles displaying almost spherical shape can be easily observed in the Zn-Zr-P coating applied to the considered stones. Moreover, the nanocomposite material seems to cover the pores on the LS surface more efficiently than plain PDMS (Figures 3a and 4a, respectively). This behavior can be observed to a lower extent even on Brick (Figures 3c and 4d, respectively). In addition, it shows how doped NPs englobed inside the polymer matrix (Figure 4b,c,e,f,h,i).

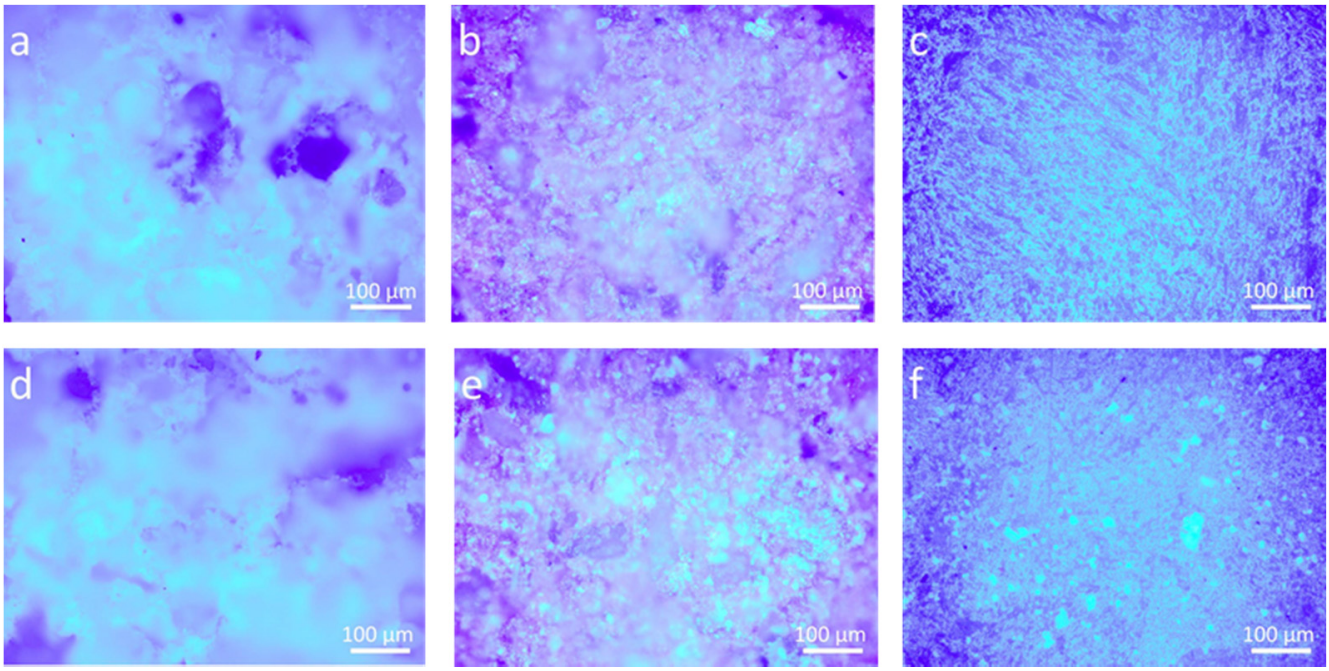

Figure 2. Optical microscope images (by UV light) of stones treated with two different coatings: (**a**) P_LS, (**b**) P_B, (**c**) P_M, (**d**) Zn-Zr-P_LS, (**e**) Zn-Zr-P_B, and (**f**) Zn-Zr-P_M.

EDS analyses were also performed in order to investigate the elemental composition of materials applied on the stone surface. The results clearly confirm that coatings labelled as P mainly contain C, O, and Si, while the nanocomposite also include Zn, and Zr, as components due to the presence of doped NPs (see inserts in Figures 3 and 4).

3.3. Durability Analyses of Protective Coatings

The main aim of this research work was to investigate the possible increased durability of the newly synthesized nano-coating and compare it with the well-known PDMS taken as the reference protecting material. The investigation of durability was performed by evaluating selective properties of both coatings after their ageing cycles as explained in the experimental section. At the end of both ageing cycles, chromatic variations, static contact angle, hardness, and self-cleaning ability (MB dye degradation under UV light) were measured, and all the results were compared to those obtained before the ageing cycles.

As indicated before, both coatings did not significantly alter the original color of stone specimens ($\Delta E^* < 5$). The data corresponding to chromatic variations are reported in Table 1, and graphically summarized in Figure 5. In general, both ageing methods did not affect very much the color of treated stones as the overall chromatic variations were below five in all the cases. Solar ageing affects to a larger extent coating on LS ($\Delta E^*_{P\_LS}$~4.8, and $\Delta E^*_{Zn\text{-}Zr\text{-}P\_LS}$~2.8) than humid chamber ageing ($\Delta E^*_{P\_LS}$~1.4, and $\Delta E^*_{Zn\text{-}Zr\text{-}P\_LS}$~0.6). On the contrary, the larger changes observed on treated brick and marble were due to the humid chamber ageing. This result could be tentatively explained on the basis of the lower porosity of B and M, which make the coating layer homogeneously distribute (NPs and polymer) on the stone surface which allow the attainment of the highly superficial layer of nano-coating on those stones due to their lower porosity with respect to the LS, which may be involved in the protection of the coating by solar ageing. In addition, the L^* coordinate became lower after humid chamber ageing in most of the cases, indicating that treated stones became little bit darker due to the humidity and temperature, while both the L^* and b^* coordinates changed due to solar ageing (Table 1).

However, we observed that, for each treated stone, plain PDMS always underwent larger color changes (about double the extent) than the nanocomposite coating, suggesting

that the newly synthesized coating displays more resistance toward ageing than the plain PDMS polymer.

On the other hand, the results of contact angle measurements showed that both coatings provide the hydrophobic nature into the stone substrates even after the two ageing processes (Table S2, in the supplementary materials).

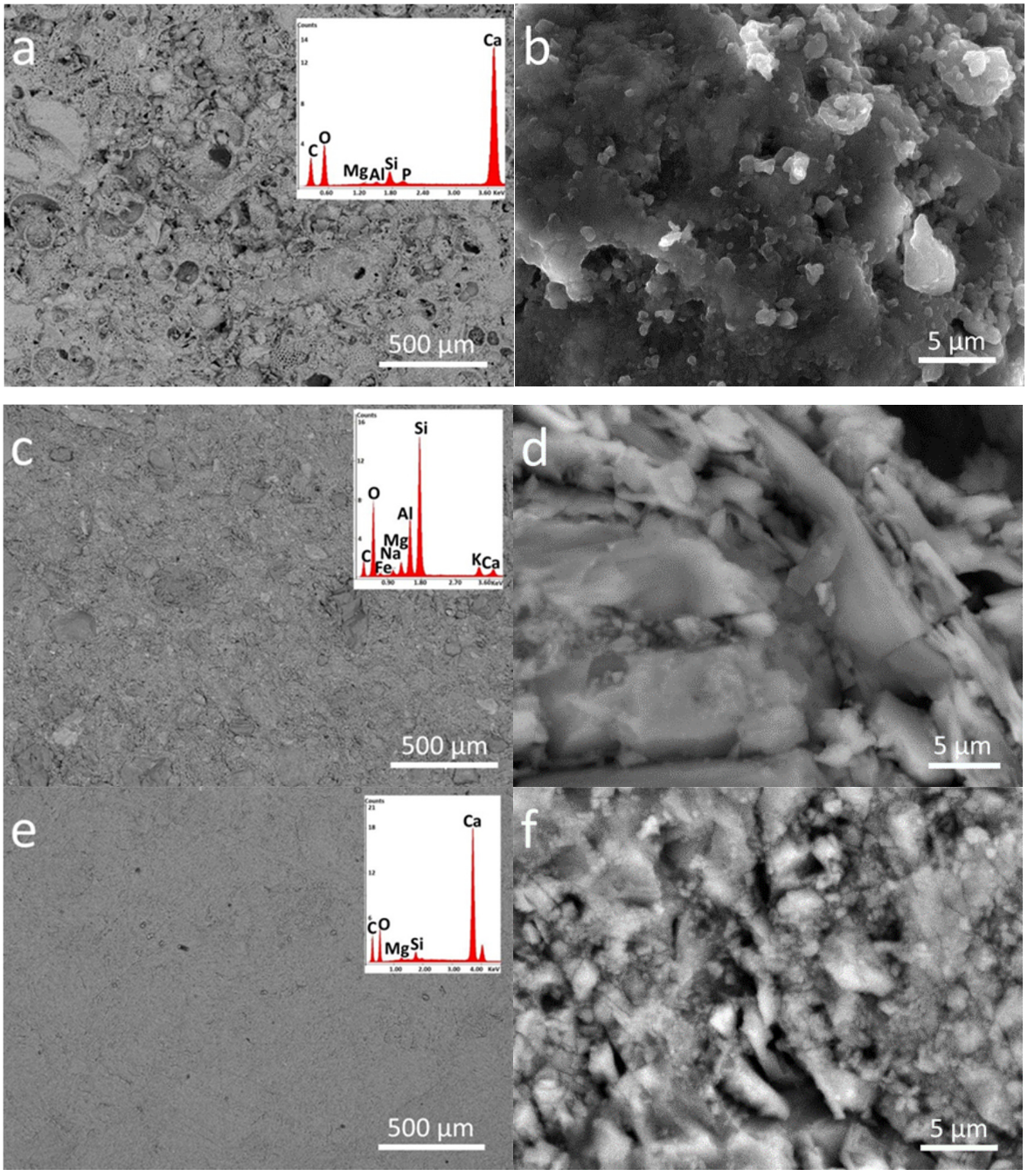

Figure 3. SEM-EDS analysis of PDMS treated stones in two different magnifications (500 µm and 5 µm): (**a**,**b**) P_LS, (**c**,**d**) P_B, and (**e**,**f**) P_M. The EDS spectra are the inset of the lower magnification images (500 µm).

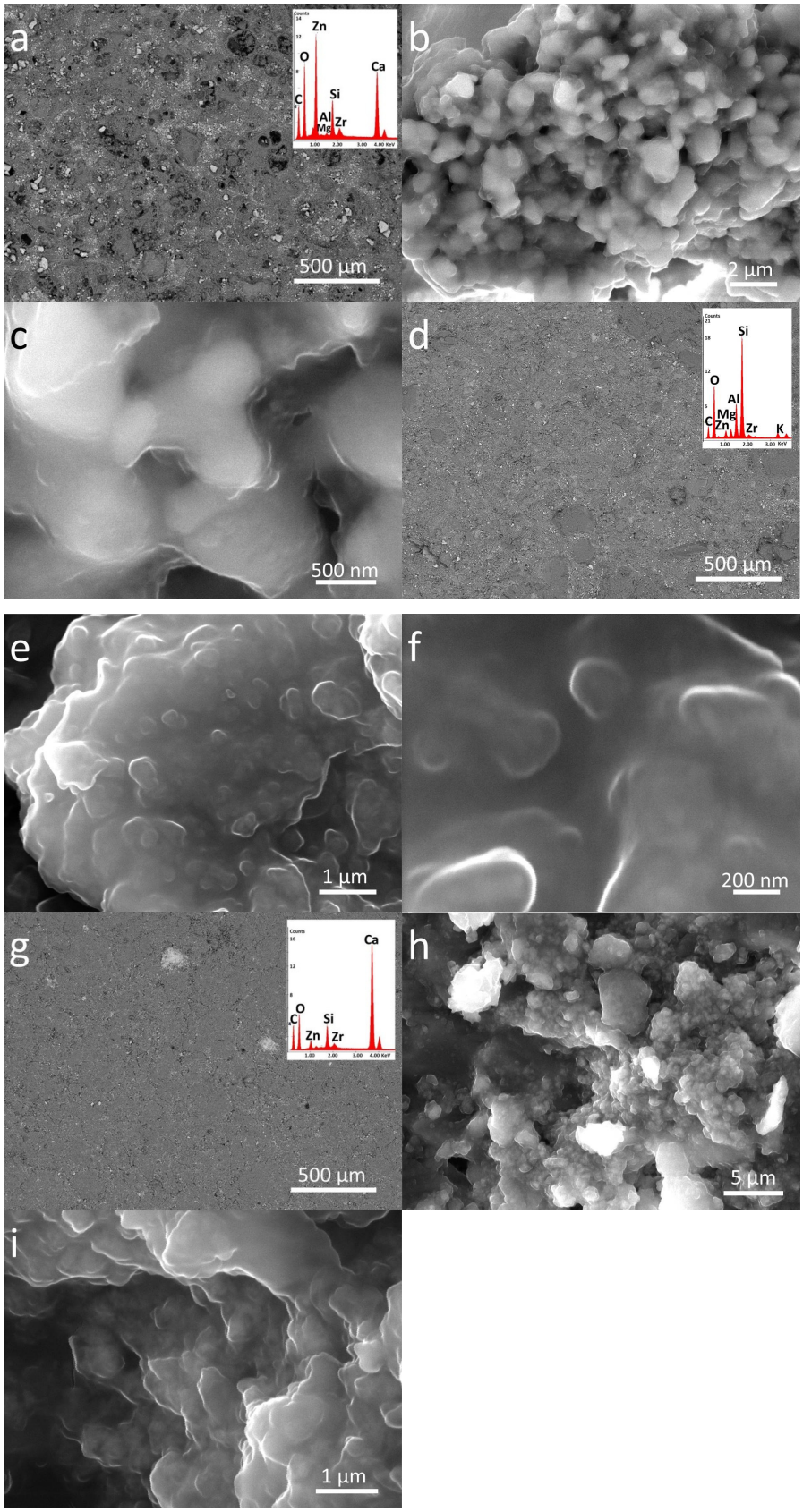

Figure 4. SEM-EDS analysis of nanocomposite treated stones in different magnifications: (**a**–**c**) Zn-Zr-P_LS, (**d**–**f**) Zn-Zr-P_B, and (**g**–**i**) Zn-Zr-P_M. The EDS spectra are the inset of the lowest magnification images (500 µm).

The surface hardness of stones due to coatings was also measured before and after ageing by performing pencil hardness tests (according to the international standard method). All the results are summarized in Table 2. Measurements performed on treating stones before ageing showed that the nanocomposite provided harder coating than the plain PDMS. In particular, the highest hardness was observed for the nanocomposite coating on the marble surface (hardness: 4H), likely because the very low porosity of the substrate induces a very high coating homogeneity. Considering the hardness of aged stone, we observed that specimens treated with PDMS in all cases underwent a hardness decrease by one level on the conventional hardness scale. On the contrary, stones treated with nanocomposite kept their unaltered hardness properties, suggesting that the presence of doped NPs in the PDMS matrix induces an increased resistance of the polymer toward ageing and, therefore, a more durable protection of the stone substrate. Interestingly, the same results were obtained independently from the two ageing processes we adopted.

Table 1. Chromatic variations of treated stones after artificial ageing cycles.

Samples	Humid Chamber Ageing (RH > 80%, T = 22 ± 3 °C)				Artificial Solar Ageing (300 W, 1000 h)			
	ΔL^*	Δa^*	Δb^*	ΔE^*	ΔL^*	Δa^*	Δb^*	ΔE^*
P_LS	−1.8 ± 0.3	1.2 ± 0.1	1.2 ± 0.2	1.4 ± 0.2	3.3 ± 0.2	−0.9 ± 0.1	−3.3 ± 0.2	4.8 ± 0.1
Zn-Zr-P_LS	−0.5 ± 0.2	0.3 ± 0	0.2 ± 0.1	0.6 ± 0.2	2.2 ± 0.1	−0.5 ± 0.1	−1.9 ± 0.3	2.8 ± 0.3
P_B	−1.6 ± 0.2	1.0 ± 0.5	1.3 ± 0.3	2.3 ± 0.5	1.7 ± 0.3	0.1 ± 0	0.1 ± 0.3	1.7 ± 0.3
Zn-Zr-P_B	−0.7 ± 0.2	−0.3 ± 0.2	−1.3 ± 0.2	1.5 ±0.1	0.3 ± 0.1	0.1 ± 0	0.1 ± 0.1	0.4 ± 0.1
P_M	−1.7 ± 0.1	−0.3 ± 0.1	−0.7 ± 0.3	1.9 ± 0.1	0.7 ± 0.2	−0.1 ± 0.2	0.2 ± 0.1	0.8 ± 0.1
Zn-Zr-P_M	−0.9 ± 0.1	−0.2 ± 0	−0.3 ± 0.2	1.0 ± 0.1	0.1 ± 0	−0.3 ± 0.1	0.2 ± 0.2	0.4 ± 0

The photodegradation effect of both coatings was examined by handling MB dye discoloration test under UV light irradiation as explained in the experimental section. First of all, the dye degradation ability of a nanocomposite coating before the ageing was investigated with respect to the plain polymer coating as shown in Figure 6a and Table 3. The effect of the self-cleaning behavior was evaluated by considering the ratios of overall chromatic variation obtained at different time intervals as well as by calculating the D^* (%) values after 48 and 96 h irradiation time. Results showed that all the stones treated with a nanocomposite coating enhanced the photodegradation effectiveness when compared to the plain PDMS-treated stones. For instance, the increment in D^* was about 20% in the case of Lecce stone and bricks treated by Zn-Zr-P, while it was 40% in the case of marble stone coated with the nanocomposite. The mechanism of MB dye degradation by NPs under UV light irradiation was clearly explained in previous papers [13,14,49] as well as the photo-absorbing capacity (UV light absorbing ability) of ZnO NPs alongside ZrO_2 NPs as good semi-conductive materials [23,24,50]. The highest discoloration effect for both treatments was observed on Marble (D* about 72, and 56% after 96 h for Zn-Zr-P, and P, respectively), likely because of the presence of a good superficial thin layer on the poorly porous stone surface, which could allow a more efficient degradation of MB dye under UV light irradiation. Notably, nanocomposite-treated stones displayed higher discoloration effects than corresponding substrates treated with plain PDMS, confirming that doped NPs considerably contribute to increase the photodegradation efficiency. The results obtained by the phtodegradation tests are in good agreement with previously reported data concerning only PDMS-treated stones [14–16,40].

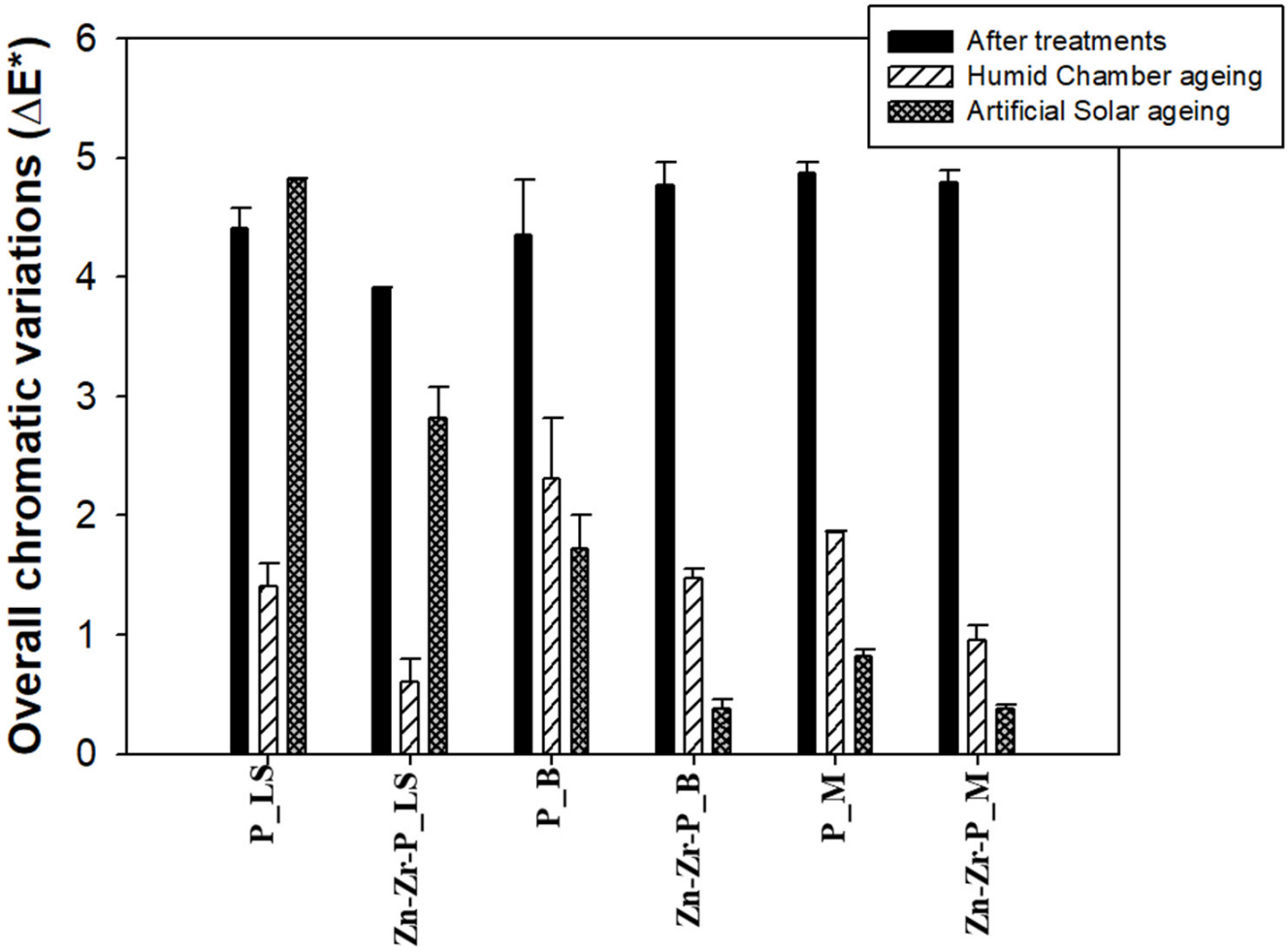

Figure 5. Overall chromatic variations of stone specimens after treatments, and after two different types of ageing cycles.

Table 2. The results of pencil hardness measurements before and after two different ageing cycles.

Samples	Before Ageing	After Artificial Ageing	
		RH > 80%, T = 22 ± 3 °C	Solar Lamp (300 W, 1000 h)
P_LS	H	F	F
Zn-Zr-P_LS	2H	2H	2H
P_B	2H	H	H
Zn-Zr-P_B	3H	2H	2H
P_M	3H	2H	2H
Zn-Zr-P_M	4H	4H	4H

As explained in the experimental section, the phtodegradation test was performed again on the treated stone that had undergone the ageing processes in order to find more information about their durability features. All the collected results are illustrated in Figure 6b,c and Figure 7a,b and Table 3. In general, the photodegradation efficiency was not affected or was affected to a low extent by both ageing procedures. In particular, it is worth noting that the photocatalytic properties (and the self-cleaning ability) exhibited by the nanocomposite coating were always distinctly better than plain PDMS and did not suffer significant reduction or decrease to a small extent even after prolonged irradiation by the solar lamp.

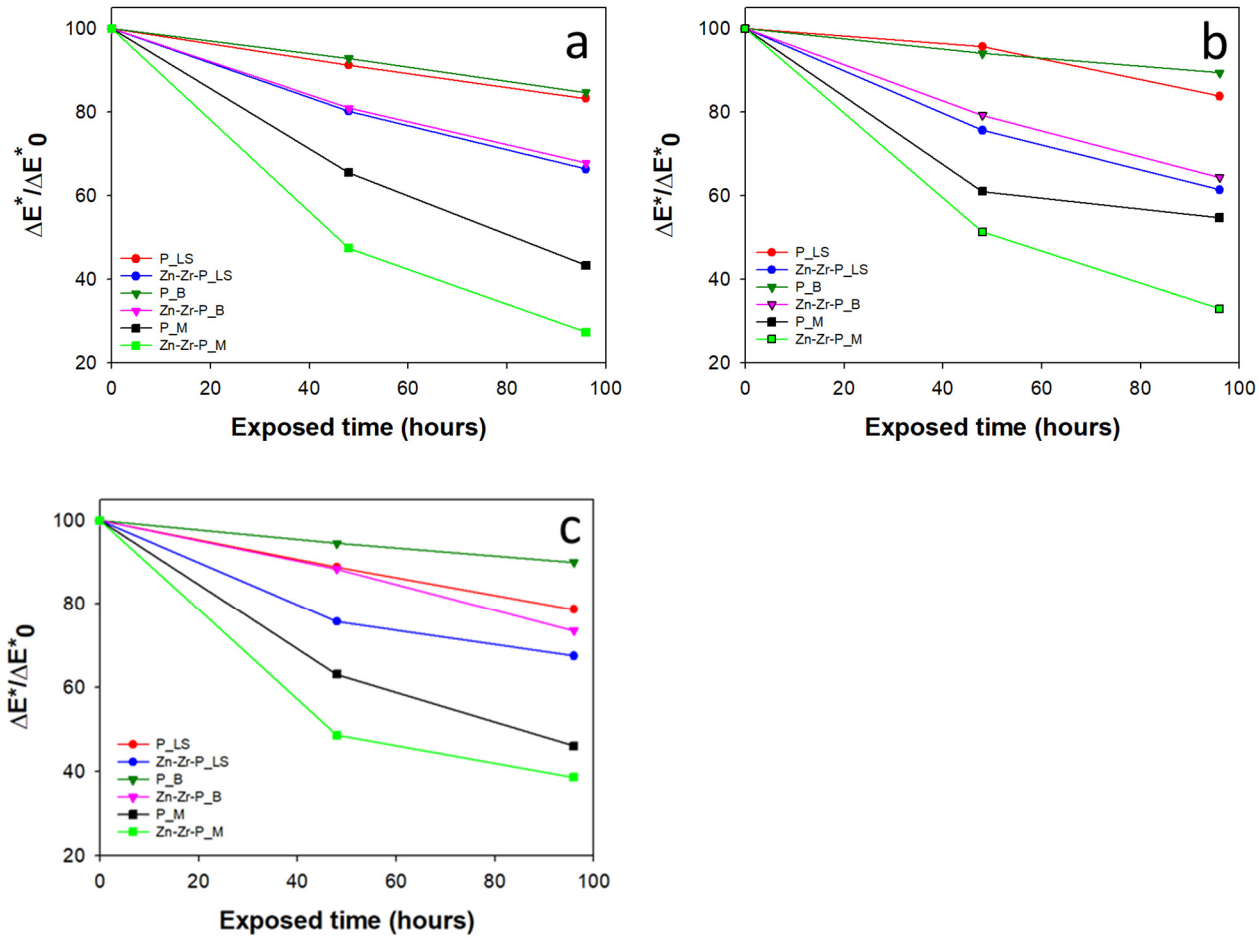

Figure 6. The photocatalytic effect of MB dye on stained stone specimens (**a**) before (**b**), and (**c**) after two different artificial ageing tests: the humid chamber, and solar lamp, respectively.

Table 3. The discoloration percentage (D^* (%)) of MB dye stains during a time of UV exposure (48 and 96 h) on treated stone samples before and after two different ageing cycles.

Samples	D^* (%)					
	Before Ageing		After Artificial Ageing Cycles			
			RH > 80%, T = 22 ± 3 °C		Solar lamp (300 W, 1000 h)	
	48 h	96 h	48 h	96 h	48 h	96 h
P_LS	15.61 ± 0.72	20.45 ± 2.01	9.80 ± 1.22	21.19 ± 0.6	12.82 ± 0.62	19.90 ± 0.13
Zn-Zr-P_LS	32.68 ± 1.53	42.90 ± 2.11	29.97 ± 2.14	44.37 ± 2.01	33.53 ± 0.96	39.37 ± 1.02
P_B	6.05 ± 3.30	13.61 ± 4.70	6.64 ± 0.79	11.03 ± 0.75	5.8 ± 0.21	13.01 ± 0.72
Zn-Zr-P_B	18.93 ± 4.55	35.52 ± 5.06	23.10 ± 1.47	34.64 ± 2.0	15.0 ± 1.31	35.03 ± 1.5
P_M	37.82 ± 2.36	55.99 ± 6.52	34.30 ± 2.79	50.37 ± 2.45	36.81 ± 2.0	54.70 ± 1.85
Zn-Zr-P_M	52.66 ± 2.04	72.25 ± 2.36	51.92 ± 3.01	68.24 ± 3.42	54.69 ± 2.5	66.70 ± 2.92

Nevertheless, the better performance can always be seen in the newly synthesized nano-coating, implying that NPs could be able to increase the photocatalytic properties (self-cleaning effect) of PDMS polymer.

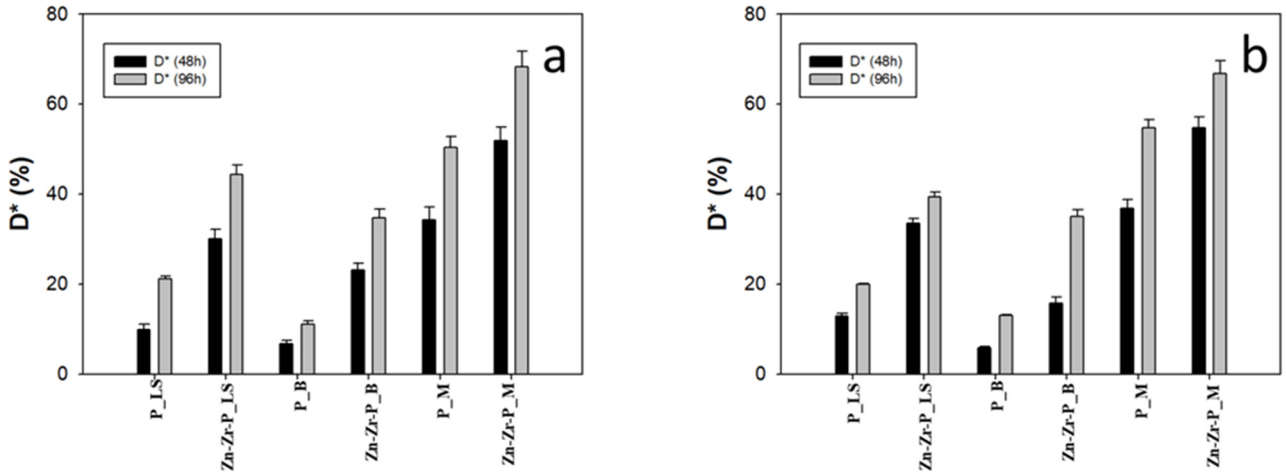

Figure 7. The MB discoloration percentage (*D** (%)) of artificially aged samples after UV light exposure (**a**) humid chamber, and (**b**) solar lamp.

4. Conclusions

The development of multi-functional and durable protective coating represents an important contribution to preserve historical artifacts. Therefore, in this research work, photo-enhanced nanocomposite coating was synthesized by in situ reaction using ZrO_2-doped ZnO with PDMS polymer. All the performances of newly prepared coating were evaluated in comparison with the well-known PDMS polymer, and their features were examined after application on three different stone substrates (LS, B, and M). All the results of considered stones highly depend on their chemical composition and porosities.

The synthesized doped NPs were spherical in shape, and displayed a 15–30 nm size range. The microscopy investigations and SEM analyses confirmed the homogeneous distribution of NPs in the polymer matrix and their englobing behavior. EDS analyses vouched for the chemical compositions of synthesized coatings, while FTIR analyses suggested possible chemical bonding between NPs and the polymer chains. The formation of chemical bonds involving the NPs' surface and the polysiloxane structure should provide an increased stability and durability compared to corresponding coatings containing only dispersed NPs.

The color changes, contact angle, capillary absorption and water vapor permeability measurements performed on both coatings indicated that the chromatic and hydric properties of the envisaged stone substrates are modified to an acceptable extent by surface treatments.

Specific experiments were performed to assess the long-term durability of the considered coatings. For this purpose, all the considered treated stones underwent two different types of ageing processes and their properties were investigated again. The results were properly compared with the results obtained before ageing, indicating that both chromatic and hydric properties are better preserved on nanocomposite-treated specimens. The hardness measurements showed that nanocomposite provided harder coating films than the plain PDMS. The hardness features of nanocomposite coatings were kept even after aging, while plain PDMS underwent a decrease in the hardness level.

Moreover, the newly synthesized nanocomposite coating exhibited a significant photocatalytic effect (self-cleaning effect) based on its ability to discolor the methylene blue dye when exposed to UV light exposure when compared to the plain polymer (PDMS). The highest efficiency was observed in the case of Marble treated with Zn-Zr-P, which displayed a discoloration factor, *D**, of 72% (*D** = 56% in the case of PDMS-treated Marble). Hence, all the results clearly explained that NPs are able to increase the photocatalytic effect of binder material (PDMS) to a good level. Additionally, both coatings mostly maintained their self-cleaning ability even after the ageing processes.

This obviously indicates that nano-coating has the better performances than PDMS in all cases and it is important to highlight that the homogeneous distribution of NPs in the polymer matrix, and their cross-linking behavior, were invoked to gain all these properties, and due to this structure NPs cannot be easily removed from the polymer chains, which can provide long-term durability. Finally, all the results are in good agreement with each other, showing that the newly synthesized nanocomposite coating can be used as a promising self-cleaning, multi-functional, and durable protective coating for different types of stones.

Supplementary Materials: The following supporting information can be downloaded at: https://www.mdpi.com/article/10.3390/chemistry4010006/s1, Table S1. The absorbed amount of products in the stone specimens, and Table S2. Contact angle measurements of treated stones before and after the ageing processes.

Author Contributions: Conceptualization, M.L.W., M.B.C. and M.L.; methodology, M.L.W. and M.B.C.; validation, M.L.W. and M.L.; formal analysis, D.S. and M.M.; investigation, M.L.W. and M.L.; resources, M.L.; data curation, M.L.W., M.B.C., D.S. and M.M.; writing—original draft preparation, M.L.W.; writing—review and editing, M.L.W. and M.L.; visualization, M.L.W.; supervision, M.L. All authors have read and agreed to the published version of the manuscript.

Funding: This research received no external funding.

Data Availability Statement: The data presented in this research study are available in the present article and in the related Supplementary Information.

Acknowledgments: The authors would like to gratefully acknowledge Ilenia Tredici for handling the SEM-EDS analysis.

Conflicts of Interest: The authors declare no conflict of interest.

References

1. Aldoasri, M.A.; Darwish, S.S.; Adam, M.A.; Elmarzugi, N.A.; Ahmed, S.M. Protecting of Marble Stone Facades of Historic Buildings Using Multifunctional TiO_2 Nanocoatings. *Sustainability* **2017**, *9*, 2002. [CrossRef]
2. Crisci, G.M.; La Russa, M.F.; Macchione, M.; Malagodi, M.; Palermo, A.M.; Ruffolo, S.A. Study of archaeological underwater finds: Deterioration and conservation. *J. Appl. Phys. A* **2010**, *100*, 855–863. [CrossRef]
3. Nugari, M.P.; Pietrini, A.M.; Caneva, G.; Imperi, F.; Visca, P. Biodeterioration of mural paintings in a rocky habitat: The Crypt of the Original Sin (Matera, Italy). *Int. Biodeterior. Biodegrad.* **2009**, *63*, 705–711. [CrossRef]
4. Sekhar, P.; Ramgir, N.; Joshi, R.; Bhansali, S. Selective growth of silica nanowires using an Au catalyst for optical recognition of interleukin-10. *Nanotechnology* **2008**, *19*, 245502–245507. [CrossRef] [PubMed]
5. Dei, L.; Salvadori, B. Nanotechnology in cultural heritage conservation: Nanometric slaked lime saves architectonic and artistic surfaces from decay. *J. Cult. Herit.* **2006**, *7*, 110–115. [CrossRef]
6. Licchelli, M.; Malagodi, M.; Weththimuni, M.; Zanchi, C. Nanoparticles for conservation of bio-calcarenite stone. *Appl. Phys. A.* **2014**, *114*, 673–683. [CrossRef]
7. La Russa, M.F.; Ruffolo, S.A.; Rovella, N.; Belfiore, C.M.; Palermo, A.M.; Guzzi, M.T.; Crisci, G.M. Multifunctional TiO_2 coatings for cultural heritage. *Prog. Org. Coat.* **2012**, *74*, 186–191. [CrossRef]
8. Weththimuni, M.L.; Licchelli, M.; Malagodi, M.; Rovella, N.; La Russa, M. Consolidation of bio-calcarenite stone by treatment based on diammonium hydrogenphosphate and calcium hydroxide nanoparticles. *Measurement* **2018**, *127*, 396–405. [CrossRef]
9. D'Arienzo, L.; Scarfato, P.; Incarnato, L. New polymeric nanocomposites for improving the protective and consolidating efficiency of tuff stone. *J. Cult. Herit.* **2008**, *9*, 253–260. [CrossRef]
10. Ricca, M.; Le Pera, E.; Licchelli, M.; Macchia, A.; Malagodi, M.; Randazzo, L.; Rovella, N.; Ruffolo, S.A.; Weththimuni, M.L.; La Russa, M.F. The CRATI project: New insights on the consolidation of salt weathered stone and the case study of San Domenico church in Cosenza (South Calabria, Italy). *Coatings* **2019**, *9*, 330. [CrossRef]
11. Manoudis, P.N.; Tsakalof, A.; Karapanagiotis, I.; Zuburtikudis, I.; Panayiotou, C. Fabrication of super-hydrophobic surfaces for enhanced stone protection. *Surf. Coat. Technol.* **2009**, *203*, 1322–1328. [CrossRef]
12. De Ferri, L.; Lottici, P.P.; Lorenzi, A.; Montenero, A.; Salvioli-Mariani, E. Study of silica nanoparticles—Polysiloxane hydrophobic treatments for stone-based monument protection. *J. Cult. Herit.* **2011**, *12*, 356–363. [CrossRef]
13. Ben Chobba, M.; Weththimuni, M.L.; Messaoud, M.; Urzi, C.; Bouaziz, J.; Leo, F.D.; Licchelli, M. Ag-TiO_2/PDMS nanocomposite protective coatings: Synthesis, characterization, and use as a self-cleaning and antimicrobial agent. *Prog. Org. Coat.* **2021**, *158*, 106342. [CrossRef]
14. Ben Chobba, M.; Weththimuni, M.L.; Messaoud, M.; Sacchi, D.; Bouaziz, J.; Leo, F.D.; Urzi, C.; Licchelli, M. Multifunctional and Durable Coatings for Stone Protection Based on Gd-Doped Nanocomposites. *Sustainability* **2021**, *13*, 11033. [CrossRef]

15. Kapridaki, C.; Pinho, L.; Mosquera, M.J.; Maravelaki-Kalaitzaki, P. Producing photoactive, transparent and hydrophobic SiO_2-crystalline TiO_2 nanocomposites at ambient conditions with application as self-cleaning coatings. *Appl. Catalyst. B Environ.* **2014**, *156–157*, 416–427. [CrossRef]
16. Crupi, V.; Fazio, B.; Gessini, A.; Kis, Z.; La Russa, M.F.; Majolino, D.; Masciovecchio, C.; Ricca, M.; Rossi, B.; Ruffolo, S.A.; et al. TiO_2–SiO_2–PDMS nanocomposite coating with self-cleaning effect for stone material: Finding the optimal amount of TiO_2. *Constr. Build. Matter.* **2018**, *166*, 464–471. [CrossRef]
17. Kapridaki, C.; Verganelaki, A.; Dimitriadou, P.; Maravelaki-Kalaitzaki, P. Conservation of Monuments by a Three-Layered Compatible Treatment of TEOS-Nano-Calcium Oxalate Consolidant and TEOS-PDMS-TiO_2 Hydrophobic/Photoactive Hybrid Nanomaterials. *Materials* **2018**, *11*, 684. [CrossRef] [PubMed]
18. La Russa, M.F.; Rovella, N.; De Buergo, M.A.; Belfiore, C.M.; Pezzino, A.; Crisci, G.M.; Ruffolo, S.A. Nano-TiO_2 coatings for cultural heritage protection: The role of the binder on hydrophobic and self-cleaning efficacy. *Prog. Org. Coat.* **2016**, *91*, 1–8. [CrossRef]
19. Luna, M.; Delgado, J.J.; Gil, M.L.A.; Mosquera, M.J. TiO_2-SiO_2 Coatings with a Low Content of AuNPs for Producing Self-Cleaning Building Materials. *Nanomaterials* **2018**, *8*, 177. [CrossRef]
20. Banerjee, S.; Dionysiou, D.D.; Pillai, S.C. Self-cleaning applications of TiO_2 by photo-induced hydrophilicity and photocatalysis. *Appl. Catalys. B Environ.* **2015**, 176–177, 396–428. [CrossRef]
21. Werf, I.D.V.D.; Ditaranto, N.; Picca, R.A.; Sportelli, M.C.; Sabbatini, L. Development of a novel conservation treatment of stone monuments with bioactive nanocomposites. *Herit. Sci.* **2015**, *3*, 29. [CrossRef]
22. Aldosari, M.A.; Darwish, S.S.; Adam, M.A.; Elmarzugi, N.A.; Ahmed, S.M. Using ZnO nanoparticles in fungal inhibition and self-protection of exposed marble columns in historic sites, Archaeol. *Anthropol. Sci.* **2019**, *11*, 3407–3422. [CrossRef]
23. Weththimuni, M.L.; Milanese, C.; Licchelli, M.; Malagodi, M. Improving the protective properties of shellac-based varnishes by functionalized nanoparticles. *Coatings* **2021**, *11*, 419. [CrossRef]
24. Weththimuni, M.L.; Capsoni, D.; Malagodi, M.; Milanese, C.; Licchelli, M. Shellac/ nanoparticles dispersions as protective materials for wood. *Appl. Phys. A* **2016**, *122*, 1058. [CrossRef]
25. Sierra-Fernandez, A.; La Rosa-García, S.C.D.; Gomez-Villalba, L.S.; Gomez-Cornelio, S.; Rabanal, M.E.; Fort, R.; Quintana, P. Synthesis, Photocatalytic, and Antifungal Properties of MgO, ZnO and Zn/Mg Oxide Nanoparticles for the Protection of Calcareous Stone Heritage. *ACS Appl. Mater. Interfaces* **2017**, *9*, 24873–24886. [CrossRef]
26. Selim, M.S.; Shenashen, M.A.; Elmarakbi, A.; Fatthallah, N.A.; Hasegawa, S.I.; El-Safty, S.A. Synthesis ultrahydrophobic thermally stable inorganic-organic nanocomposites for self-cleaning foul release coatings. *Chem. Eng. J.* **2017**, *320*, 653–666. [CrossRef]
27. Weththimuni, M.L.; Ben Chobba, M.; Tredici, I.; Licchelli, M. Polydimethylsiloxane (PDMS)/ZrO2-doped ZnO nanocomposites as Protective Coatings for Stone Materials, TC4 MetroArchaeo 2020-IMEKO TC4 International Conference on Metrology for Archaeology and Cultural Heritage. 2020, pp. 527–531. Available online: https://www.imeko.org/publications/tc4-Archaeo-2020/IMEKO-TC4-MetroArchaeo2020-100.pdf (accessed on 7 December 2021).
28. Singh, A.K.; Nakate, U.T. Microwave synthesis, characterization, and photoluminescence properties of nanocrystalline zirconia. *Sci. World J.* **2014**, *2014*, 349457. [CrossRef]
29. Ha, T.T.; Canh, T.D.; Tuyen, N.V. A Quick Process for Synthesis of ZnO Nanoparticles with the Aid of Microwave Irradiation. *ISRN Nanotech.* **2013**, *2014*, 497873. [CrossRef]
30. *UNI 10921:2001*; Beni culturali—Materiali lapidei naturali ed artificiali—Prodotti idrorepellenti. Applicazione su Provini e Determinazione in Laboratorio delle loro Caratteristiche: Milan, Italy, 2001.
31. Weththimuni, M.L.; Crivelli, F.; Galimberti, C.; Malagodi, M.; Licchelli, M. Evaluation of commercial consolidating agents on very porous biocalcarenite. *Int. J. Conserv. Sci.* **2020**, *11*, 251–260.
32. *UNI EN 15886:2010*; Conservation of cultural property—Test methods. Colour Measurement of Surfaces: Milan, Italy, 2010.
33. *UNI EN 15802:2010*; Conservazione dei Beni culturali-Metodi di Prova-Determinazione dell'Angolo di Contatto Statico. UNI Ente Italiano di Unificazione: Milan, Italy, 2010.
34. *UNI EN 15801:2010*; Conservazione dei Beni Culturali, Metodi di Prova, Determinazione Dell'assorbimento Dell'acqua per Capillarità. UNI: Milan, Italy, 2010.
35. *UNI EN 15803:2010*; Conservazione dei Beni Culturali, Metodi di Prova, Determinazione Della Permeabilità al Vapore D'acqua. UNI: Milan, Italy, 2010.
36. *ISO 15184:1998*; Paints and Varnishes—Determination of Film Hardness by Pencil Test. International Organization for Standardization: Genève, Switzerland, 1998.
37. Quagliarini, E.; Bondioli, F.; Goffredo, G.B.; Cordoni, C.; Munafò, P. Self-cleaning and de-polluting stone surfaces: TiO_2 nanoparticles for limestone. *Constr. Build. Mater.* **2012**, *37*, 51–57. [CrossRef]
38. Ariati, R.; Sales, F.; Souza, A.; Lima, R.A.; Ribeiro, J. Polydimethylsiloxane Composites Characterization and Its Applications: A Review. *Polymers* **2021**, *13*, 4258. [CrossRef] [PubMed]
39. Bodas, D.; Khan-Malek, C. Formation of more stable hydrophilic surfaces of PDMS by plasma and chemical treatments. *Microelectron. Eng.* **2006**, *83*, 1277–1279. [CrossRef]
40. Kapridaki, C.; Maravelaki-Kalaitzaki, P. TiO_2–SiO_2–PDMS nano-composite hydrophobic coating with self-cleaning properties for marble protection. *Prog. Org. Coat.* **2013**, *76*, 400–410. [CrossRef]

41. Peroz, C.; Chauveau, V.; Barthel, E.; Søndergård, E. Nano Imprint Lithography on Silica Sol-gels: A simple route to sequential patterning. *Adv. Mater.* **2009**, *21*, 555–558. [CrossRef] [PubMed]
42. Guo, Z.; Wei, S.; Shedd, B.; Scaffaro, R.; Ereira, T.; Hahn, H. Particles surface engineering effect on the mechanical, optical and photoluminescent properties of ZnO/vinyl-ester resin nanocomposites. *J. Mater. Chem.* **2007**, *17*, 806–813. [CrossRef]
43. Chandra Babu, B.; Naresh, V.; Jaya Prakash, B.; Buddhudu, S. Structural, Thermal and Dielectric Properties of Lithium Zinc Silicate Ceramic Powders by Sol-Gel Method. *Ferroelectr. Lett.* **2011**, *38*, 114–127. [CrossRef]
44. Licchelli, M.; Marzolla, S.J.; Poggi, A.; Zanchi, C. Crosslinked fluorinated polyurethanes for the protection of stone surfaces from graffiti. *J. Cult. Herit.* **2011**, *12*, 34–43. [CrossRef]
45. Licchelli, M.; Malagodi, M.; Weththimuni, M.; Zanchi, C. Anti-graffiti nanocomposite materials for surface protection of a very porous stone. *Appl. Phys. A* **2014**, *116*, 1525–1539. [CrossRef]
46. Wang, C.-Z.; Chen, A.-J.; Li, Z.-Q.; Gong, C.-A.; Wang, S.; Yan, W.-M. Experimental and numerical investigation on penetration of clay masonry by small high-speed projectile. *Def. Technol.* **2021**, *17*, 1514–1530. [CrossRef]
47. Sassoni, E.; Franzoni, E. Influence of porosity on artificial deterioration of marble and limestone by heating. *Appl. Phys. A: Mater. Sci. Process.* **2014**, *115*, 809–816. [CrossRef]
48. Licchelli, M.; Malagodi, M.; Weththimuni, M.L.; Zanchi, C. Water-repellent properties of fluoroelastomers on a very porous stone: Effect of the application procedure. *Prog. Org. Coat.* **2013**, *76*, 495–503. [CrossRef]
49. Ben Chobba, M.; Messaoud, M.; Weththimuni, M.L.; Bouaziz, J.; Licchelli, M.; Leo, F.D.; Urzì, C. Preparation and characterization of photocatalytic Gd-doped TiO_2 nanoparticles for water treatment. *Environ. Sci. Pollut. Res.* **2019**, *26*, 32734–32745. [CrossRef] [PubMed]
50. Weththimuni, M.L.; Capsoni, D.; Malagodi, M.; Licchelli, M. Improving Wood Resistance to Decay by Nanostructured ZnO-Based Treatments. *J. Nanometer.* **2019**, *2019*, 6715756. [CrossRef]